# Learning control algorithm for nonlinear maps

Jair Botina and Herschel Rabitz
*Department of Chemistry, Princeton University, Princeton, New Jersey 08544*
(Received 2 June 1997)

A feedback optimal control algorithm is developed for $N$-dimensional maps, which uses learning-based feedback optimal control techniques. The algorithm has two steps: (1) Learn the control of a reference map containing a stochastic term. (2) Apply the learned control to the laboratory system employing real time feedback. The stochastic component of the learning step is important to provide a close knit family of controls to handle laboratory uncertainty and noise. As an example, the formalism is applied to simulated two- and three-dimensional nonlinear laboratory maps in the presence of noise. [S1063-651X(97)11309-5]

PACS number(s): 05.45.+b

## I. INTRODUCTION

Ott, Grebogi, and Yorke [1] proposed a method for controlling systems described by dynamical maps. Their method consists of first choosing an unstable periodic orbit embedded in the chaotic dynamics, and then defining a small region around the desired periodic orbit. One needs to evolve the dynamical map for each initial condition (usually chosen at random) in the desired small region. Then a suitable small perturbation of the control parameter is applied in order to force the trajectory to stay around the desired unstable periodic orbit. This technique has been applied to a wide variety of experimental systems [2]. Other methods have been proposed including a continuous feedback approach [3], a statistical analysis technique [4], a local response algorithm [5], geometric resonance [6], etc. These methods suggest that there is flexibility in the control of nonlinear dynamics.

Here we present an approach for nonlinear control, where we use learning-based feedback optimal control techniques in order to determine the external control interaction $\epsilon_n$ and/or model parameters $p_n$ (accessible parameters within the map) at discrete times $n=1,2,\ldots$. In some cases $p_n$ and $\epsilon_n$ may reduce to the same control variables. The algorithm does not require intricate knowledge of the laboratory dynamical system. The method starts with a known $N$-dimensional reference dynamical system and a specific cost functional. The reference system should ideally be closely related to the true one of interest in the laboratory, but the demand here is not high. A stochastic driving term is added to the reference model which greatly enhances the scope and robustness of the learned control for transfer to the actual laboratory system. The latter transfer constitutes the second step for laboratory implementation (studied under simulation here).

## II. LEARNING CONTROL

We assume that the experimentally observable state $\mathbf{X}$ of a system can be represented by an $N$-dimensional nonlinear map. Although we often do not precisely know the true map $\tilde{\mathbf{F}}$, we assume that the following reasonable reference representation

$$\mathbf{X}_{n+1}=\mathbf{F}(\mathbf{X}_n,p_n,\epsilon_n,\xi_n) \tag{1}$$

is available. Here $\xi_n$ is a random disturbance (i.e., noise) which serves the special purpose of broadening the scope of the learned control of the reference map $\mathbf{F}$ in preparation for transfer to the laboratory where the true map $\tilde{\mathbf{F}}$ may be somewhat different. Although the map is specified at discrete points $n$, below we will refer to these equivalently as a time variable.

The first step is to learn control with the reference map utilizing optimal control theory. Optimal control theory is based on constructing a minimizing cost functional operative during the control process. The learning control algorithm assumes *a priori* the existence of local control over a small time interval specified by a window of $n_p$ discretized time points. We formulate local control by prescribing a cost functional $J_i$ for the $i$th interval spanned by the $n_p$ time points. The functional is defined such that its minimization with respect to the control $\epsilon_n$ and model parameter $p_n$ with $(i-1)n_p \leq n \leq in_p$ meet the physical objective as best as possible. The total cost functional is given by

$$J=\sum_{i=1}^{n_d} J_i, \tag{2}$$

where the evolution dynamics can be done as long is desired by extending the number of control intervals $n_d$. The breaking of $J$ into pieces $J_i$ for individual minimization as the goal of stabilization reflects the local control structure in chaotic systems or ones containing a significant level of noise. This local approach is a key simplifying feature of the problem. The cost functional $J_i$ for each interval is

$$J_i=\sum_{j=n_i+1}^{in_p} f(\mathbf{X}_j)+\omega_1\sum_{j=n_i+1}^{in_p}\epsilon_j^2+\omega_2\sum_{j=n_i+1}^{in_p}p_j^2, \qquad i=1,\ldots, \tag{3}$$

where $\omega_1$ and $\omega_2$ are positive constant weights, $n_i=(i-1)n_p$ and $f(\mathbf{X}_j)$ is a positive definite function that acts to guide the dynamics to the controlled objective state (e.g., achieving a periodic orbit, driving the chaotic dynamics to a specific target region, maintaining chaos, etc). The weights $\omega_1$ and $\omega_2$ act as penalties to keep the magnitude of the controls as small as possible [7].

 

We need to minimize the cost functional $J_i$ by an appropriate search for $\epsilon_n$ and/or $p_n$, subject to the constraint that Eq. (1) is satisfied. Many means can be applied for this task, and here we illustrate perhaps the simplest approach. Considering the $i$th interval in Eq. (3), we prescribe $n_c$ uniform values of $\epsilon_n$ and/or $p_n$ for each of the $n_p$ time points. A particular configuration of controls for the $i$th interval is provided by the set of $n_p$ values for $\epsilon_n$ and/or $p_n$ over $(i-1)n_p \leqslant n \leqslant in_p$. Each of the possible $n_c$ values for $\epsilon_n$ and/or $p_n$ is scaled by an overall parameter $\alpha$. The total number of configurations in the $i$th interval is $(n_c)^{n_p}$. As an example, for the limiting case of the $i$th interval having only one point (i.e., $n_p=1$) and with $n_c=3$ there are three possible values of $\epsilon_j$ and/or $p_j$ constituting the configuration:

$$\begin{matrix}1\\2\\3\end{matrix}\begin{pmatrix}\alpha\\0\\-\alpha\end{pmatrix}. \tag{4}$$

The index 1, 2, or 3 labels the possible configurations of the control. In this limiting case the control can take on any of the values $\alpha, 0, -\alpha$ in the $i$th interval. For $n_p=1$ and $n_c=5$ there are five configurations:

$$\begin{matrix}1\\2\\3\\4\\5\end{matrix}\begin{pmatrix}2\alpha\\\alpha\\0\\-\alpha\\-2\alpha\end{pmatrix}. \tag{5}$$

Again, this case represents only one local control $n_p=1$ with five possible values. For $n_p=2$ and $n_c=3$ there are $3^2=9$ possible configurations, each consisting of a pair of control values:

$$\begin{matrix}1\\2\\3\\4\\5\\6\\7\\8\\9\end{matrix}\begin{pmatrix}\alpha&\alpha\\\alpha&0\\\alpha&-\alpha\\0&\alpha\\0&0\\0&-\alpha\\-\alpha&\alpha\\-\alpha&0\\-\alpha&-\alpha\end{pmatrix}. \tag{6}$$

For example, the third configuration in the $i$th interval has field value $\alpha$ at the first time point and field value $-\alpha$ at the second time point.

Each of the total number $(n_c)^{n_p}$ of configurations is evaluated for its degree of successful control by substituting the dynamical system containing a configuration for testing, described by Eq. (1), into the cost functional Eq. (3) at each instant of discrete time. As an illustration for the case of Eq. (4) with $p_n=0$, we have

$$J_{i=1}=\begin{pmatrix}f(\mathbf{X}_1^{\alpha})+\omega_1\alpha^2\\f(\mathbf{X}_1^{0})\\f(\mathbf{X}_1^{-\alpha})+\omega_1\alpha^2\end{pmatrix}, \tag{7}$$

where the superscript $\alpha$ on $\mathbf{X}$ indicates that $\mathbf{X}$ is evaluated at control values scaled with $\alpha$. For Eq. (6), we have

$$J_{i=1}=\begin{pmatrix}f(\mathbf{X}_1^{\alpha})+f(\mathbf{X}_2^{\alpha})+2\omega_1\alpha^2\\f(\mathbf{X}_1^{\alpha})+f(\mathbf{X}_2^{0})+\omega_1\alpha^2\\f(\mathbf{X}_1^{\alpha})+f(\mathbf{X}_2^{-\alpha})+2\omega_1\alpha^2\\f(\mathbf{X}_1^{0})+f(\mathbf{X}_2^{\alpha})+\omega_1\alpha^2\\f(\mathbf{X}_1^{0})+f(\mathbf{X}_2^{0})\\f(\mathbf{X}_1^{0})+f(\mathbf{X}_2^{-\alpha})+\omega_1\alpha^2\\f(\mathbf{X}_1^{-\alpha})+f(\mathbf{X}_2^{\alpha})+2\omega_1\alpha^2\\f(\mathbf{X}_1^{-\alpha})+f(\mathbf{X}_2^{0})+\omega_1\alpha^2\\f(\mathbf{X}_1^{-\alpha})+f(\mathbf{X}_2^{-\alpha})+2\omega_1\alpha^2\end{pmatrix}. \tag{8}$$

Each of the values of $J_1$ [e.g., in Eq. (8)] would be tested to determine the smallest value to identify the best configuration. The corresponding control value would be chosen and then a move taken to $i=2, \ldots,$ etc. In some cases the value of $\alpha$ would be changed to attempt a better solution. The generalization to include a model parameter $p_n$, or other control parameters implicit in the nonlinear map, is straightforward.

The minimization procedure permits the determination of the best case among all the configurations for the external control or model parameter. For some choices of $f(\mathbf{X})$ it can happen that a starting $\alpha$ value may not yield a minimum for the cost functional. In this case the $\alpha$ value must be increased until $J_i$ has at least one minimum, determining the controlled state over the $i$th interval $\mathbf{X}_n$, $\mathbf{X}_{n+1}, \ldots,$ $\mathbf{X}_{n+n_p-1}$ with its corresponding discrete control function $\epsilon_n, \epsilon_{n+1}, \ldots, \epsilon_{n+n_p-1}$, and $n=(i-1)n_p+1$ from Eq. (3). This process is repeated for the next interval $i+1$ and propagated as long as desired. We will show in some illustrations that small values for $n_p$ and $n_c$ are typically sufficient to achieve the desired control objective. The role of the stochastic term $\xi_n$ deserves special comment, as without $\xi_n$ the two steps (1) learning control and (2) laboratory application will not likely succeed. The term $\xi_n$ serves to broaden out the region of the state space sampled by the map, and hence provides a more robust repertoire of controls $\epsilon_n, n=1, \ldots$ to draw upon to stabilize or generally guide the map to achieve its controlled evaluation. For this purpose it is generally only necessary to treat $\xi_n$ as a single particular random sequence (trajectory) over $n=1,2, \ldots$ to provide the desired sampling.

## III. REAL TIME FEEDBACK

The second step in the process is to apply the learned control $\epsilon_n$ and $p_n$ to the laboratory system. However, this can not be simply done by a direct application of the sequence $\epsilon_1, \epsilon_2, \ldots, \epsilon_n, \epsilon_{n+1}, \ldots$ due to laboratory noise and lack of precise knowledge about the laboratory map. We operate in the following manner. Each learned state set $\mathbf{X}_n, \mathbf{X}_{n+1}, \ldots, \mathbf{X}_{n+n_p-1}$ in the $i$th interval with $n=(i-1)n_p+1$ has a particular sequence of controls $\epsilon_n, \ldots, \epsilon_{n+n_p-1}$ associated with it. In the laboratory at the

current time step we may observe the state as $\tilde{\mathbf{X}}$, and the task is to identify the appropriate controls to apply from the learned set. Thus we seek to find the learned state $\mathbf{X}_n$ that is close to $\tilde{\mathbf{X}}$,

$$\lfloor n \rfloor = \min |\tilde{\mathbf{X}} - \mathbf{X}_n|, \tag{9}$$

where $\lfloor n \rfloor$ indicates the index $n$ at which the minimum condition is satisfied. The index $\lfloor n \rfloor$ is used to specify the values of the controlled sequence as $\epsilon_{\lfloor n \rfloor}, \epsilon_{\lfloor n \rfloor + 1}, \ldots, \epsilon_{\lfloor n \rfloor + n_p - 1}$ to be applied. The process is then repeated with a new observation of $\tilde{\mathbf{X}}$. It is important to understand that the net application of Eq. (9) can draw on the entire set of learned dynamics (i.e., the control over the interval may not actually start with $\epsilon_{\lfloor n \rfloor + n_p}$ due to laboratory noise and uncertainty).

To summarize, the algorithm for controlling an $N$-dimensional map consists of two general steps I and II.

(I) Learn control of a stochastically driven reference map **F**.

(a) Choose a random initial starting point $X_0$ and the values of $n_p$ and $n_c$.

(b) Minimize the cost functional in Eq. (3) over the control configurations using the observed results of the map.

(c) If a minimum solution for $J_i$ is not found among all the configurations, then increase $\alpha \rightarrow \alpha + \delta$, where $\delta$ is small, and repeat step (b).

(d) Return to step (b) for the next interval $i$ until a desired number of steps is completed.

(II) Apply the learned control in part I to the laboratory map.

(a) Observe the current laboratory state $\tilde{\mathbf{X}}$ and seek the learned state $\mathbf{X}_{\lfloor n \rfloor}$ closest to it.

(b) Apply the control sequence $\epsilon_{\lfloor n \rfloor}, \epsilon_{\lfloor n \rfloor + 1}, \ldots, \epsilon_{\lfloor n \rfloor + n_p - 1}$, and observe the final outcome $\tilde{\mathbf{X}}'$.

(c) Return set (a) with $\tilde{\mathbf{X}} \rightarrow \tilde{\mathbf{X}}'$, and repeat as many times as desired.

The simplicity of this algorithm for a laboratory dynamical map is evident from the fact it does not require identifying the unstable periodic orbits, performing a local stability analysis, determining a basin of attraction, etc. The algorithm detects periodic unstable points to control chaotic motion, and addresses the irregular dynamics around a region where it is most likely to control the chaotic dynamics with a minimum magnitude control perturbation. If a stable orbit exists in the unperturbed system (i.e., $\epsilon_n = 0$) consistent with $\min f(\mathbf{X})$, then the cost function will be biased toward such a solution [7] as a result of the penalty terms weighted by $\omega_1$ in Eq. (3).

## IV. NUMERICAL EXAMPLES

In the following examples, we consider only control through an external interaction which demonstrates that such an interaction can stabilize the chaotic dynamics.

### A. Learn control of the reference map

As a first example, consider the two-dimensional Hénon map [8]

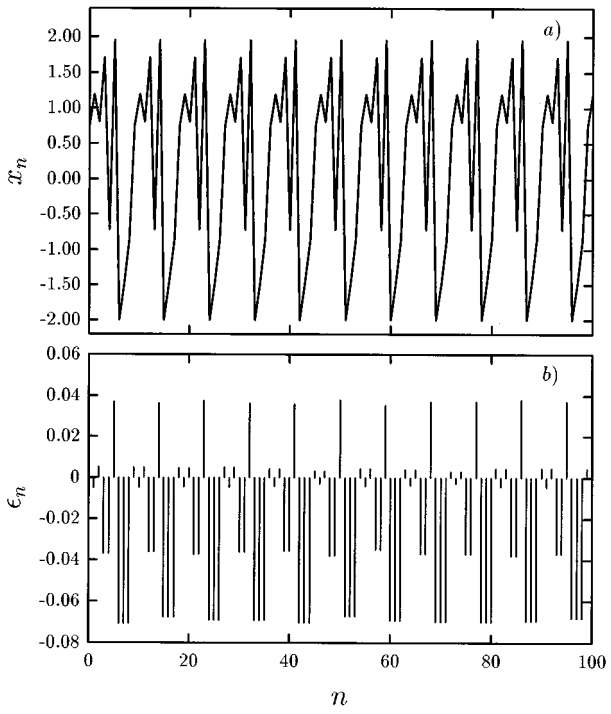


FIG. 1. Stabilization of chaotic dynamics in a two-dimensional Hénon map with noise. (a) Control of the state $x_n$ vs map index $n$. (b) Optimal external interaction $\epsilon_n$ needed to preserve the periodic motion in (a).

$$x_{n+1} = p - x_n^2 + 0.3 y_n + \epsilon_n + \xi_n,$$
$$y_{n+1} = x_n, \tag{10}$$

where the critical parameter $p = p_c$ has the value $\sim 1.42$; for $p > p_c$, the map dynamics is chaotic. Here we chose the value $p = 2.0$ beyond criticality, and $\xi_n$ is Gaussian white noise with zero mean and standard deviation $\xi = 1 \times 10^{-3}$ [9]. This system, without noise, was chosen earlier to study anticontrol [8] with potential applications in biological disorder (the proper operation of some systems seems to demand chaotic and/or complex dynamics) [10].

The function $f(x_n, y_n, p)$ in the cost functional $J_i$ that minimizes the deviation of the chaotic trajectory for each interval $i$ was

$$f(x_n, y_n, p) = \begin{cases} 0 & \text{if } x_n, y_n \subset \mathcal{R} \\ 1 \times 10^5 & \text{if } x_n, y_n \not\subset \mathcal{R}, \end{cases} \tag{11}$$

where $\mathcal{R}$ is a specific target region for motion of the dynamical system. The region $\mathcal{R}$ may be made more restrictive in an iterative fashion as the control evolves. The weight parameters were chosen as $\omega_1 = \omega_2 = 1$. The number of discrete time intervals was $n_p = 3$ and $n_c = 3$, so we have 27 search configurations. The low number of configurations was found to be sufficient to stabilize the chaotic dynamics using a small control perturbation $\epsilon_n$ (for the Hénon map, control through $p_n$ and $\epsilon_n$ are equivalent). The periodic unstable points are unknown in this approach, but it is not necessary to know them in order to control the chaotic dynamics. The region $\mathcal{R}$, was originally specified as $-2.2 \leqslant \mathcal{R} \leqslant 2.2$ for both $x_n$ and $y_n$, which produces similar anti-control dynamics as

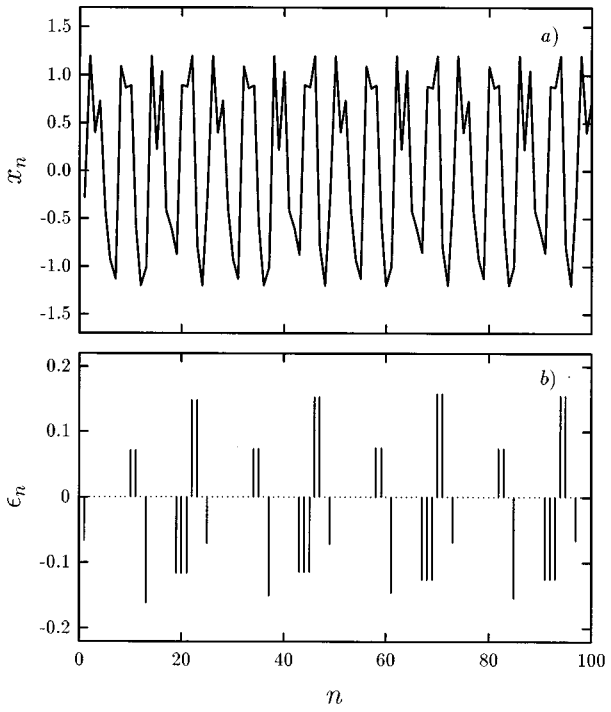


FIG. 2. Stabilization of chaotic dynamics in a three-dimensional map with noise (the same Gaussian white noise as in the two-dimensional map of Fig. 1). (a) Control of the state $x_n$ vs map index $n$. (b) Optimal external interaction $\epsilon_n$ needed to preserve the periodic motion in (a).

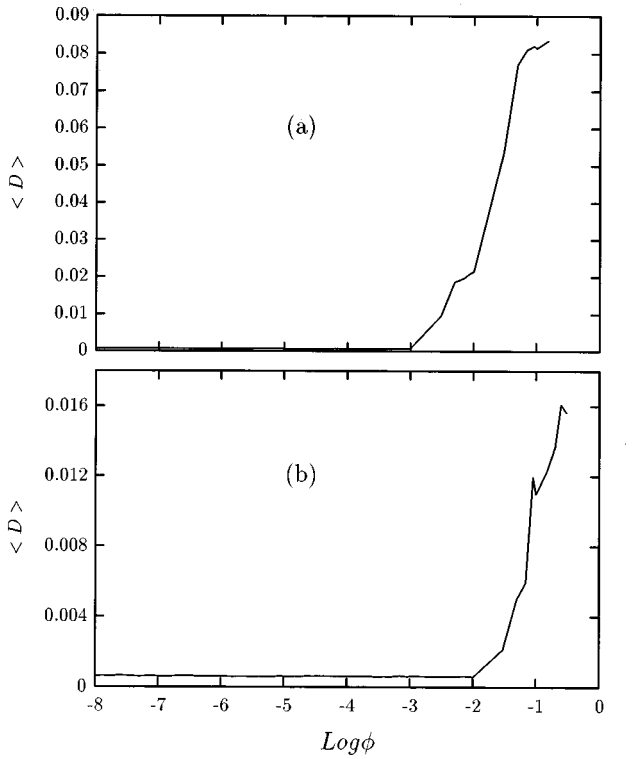


FIG. 3. Average deviation $\langle D \rangle$ of the laboratory and learned trajectories with respect to Gaussian white noise in the optimal control field sequence and the initial conditions. The noise is characterized by its standard deviation $\phi$. $\langle D \rangle$ is defined as $\langle D \rangle = (1/MN_T)\Sigma_{m,n=1}^{MN_T}|\tilde{\mathbf{X}}_n^m - \mathbf{X}_n|$ which measures the deviation from the reference controlled trajectory $\mathbf{X}_n$ given in Fig. 2, and the new observed control trajectory $\tilde{\mathbf{X}}_n^m$ generated by Eq. (9) for the $m$th member of an ensemble with $M$ terms (in both cases $M=100$). $N_T=2000$ is the number of controlled discrete time steps. (a) $\phi$ is noise in the optimal control sequence. (b) $\phi$ is noise in the initial condition ($X_0 = X_0 + \phi$).

in Fig. 12 of the work by Yang *et al.* [8]. The region $\mathcal{R}$ was then redefined to be a tight envelope around the phase plane curve. This new region $\mathcal{R}$ is used in order to predict the new external interaction and to stabilize the system around periodic unstable points. This gives a set of controlled points around the unstable periodic point.

Figure 1 shows a portion of the learned control dynamics in which the total number of intervals $1 \leqslant i \leqslant n_d$ was $n_d = 300$. We show the regular dynamics of the state $x_n$, along with the optimal external interaction $\epsilon_n$ needed to preserve regular dynamics, with a single Gaussian white noise trajectory of standard deviation $1 \times 10^{-3}$. It is evident that the control field in the presence of the noise trajectory produces periodic motion of the system. The slightly nonperiodic nature of the control in Fig. 1 is significant, and it results from the noise in the system. The total number of periodic unstable points are nine, in which the control field forces the chaotic dynamics to move.

As a second example, consider a three-dimensional map [11]

$$x_{n+1} = a x_n y_n - b z_n + (b-1) z_n^3 + \epsilon_n + \xi_n,$$

$$y_{n+1} = x_n,$$

$$z_{n+1} = y_n, \tag{12}$$

where $a = 0.2$ and $b = 2.38$. When $\epsilon_n = 0$ and $\xi_n = 0$, these parameters produce hyper$^2$-chaos (three positive Lyapunov characteristic exponents) dynamics [11]. The external interaction $\epsilon_n$ is used as a control with the objective of stabilizing the chaotic dynamics and localizing the unstable periodic points. The total number of configurations was 27, with $n_p = 3$ and $n_c = 3$, as for the two-dimensional map. It is interesting that for successful control the number of points $n_p$ and $n_c$ does not directly depend on the dimensionality of the map. The value of $-1.2 \leqslant \mathcal{R} \leqslant 1.2$ was chosen to predict the periodic motion of the three-dimensional map.

Figure 2 shows the results for a portion of the dynamics of the proposed algorithm for the three-dimensional case, in which the total number of intervals was $n_d = 300$. We show the regular dynamics of the state $x_n$ with the optimal external interaction $\epsilon_n$ needed to preserve regular dynamics. Similar periodic dynamics are found for the state components $y_n$ and $z_n$. The number of periodic unstable points associated with the chaotic dynamics is 24.

### B. Application of the learned control to a laboratory map

Figures 1 and 2 show the learned controlled dynamics through an external control interaction in the presence of imposed noise trajectory. Here through simulation we will show that the learned control field can be applied to achieve laboratory control. Figures 3 and 4 show the robustness of the present approach with respect to small errors on the op-

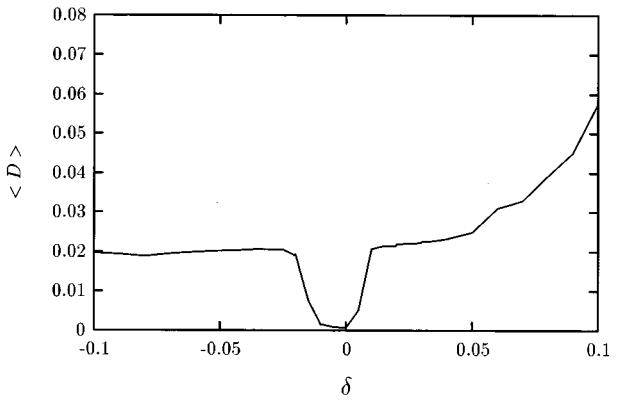


FIG. 4. Robustness of the present learning control with respect to uncertainty in the control parameter $b$ for the three-dimensional map $b=b_{\mathrm{ref}}+\delta$. The reference learning control dynamics has the value $b_{\mathrm{ref}}=2.38$ as in Fig. 2.

timal control field sequence [Fig. 3(a)], initial conditions [Fig. 3(b)], and uncertainty in the parameters (Fig. 4) of the three-dimensional map. Similar results were found for the two dimensional map. We started with the same control trajectory in Fig. 2, and introduced small deviations in either the initial conditions, control field sequence, or uncertainty in the map parameters. The noise ensemble had 100 members, and 2000 discrete time steps were followed. In the figures (see the caption to Fig. 3) $\langle D \rangle$ measures the deviation of the simulated laboratory control trajectory from the trajectory in Fig. 2. The proposed algorithm can support small errors in the optimal control field sequence of the order of $1\times10^{-3}$, in the initial conditions of the order of $1\times10^{-2}$, and uncertainty in the $b$ parameter of approximately $5\times10^{-2}$ for this example. The controlled motion appears periodic as in Fig. 2 for this interval of errors, but the motion becomes irregular and diverges for larger values of disturbance. These simulation results show the degree of robustness of the present algorithm for potential application in the laboratory. We emphasize that the presence of noise $\xi_n$ in the learning process is critical for obtaining robustness, as without $\xi_n$ there is essentially no tolerance to laboratory errors and uncertainty.

## V. CONCLUSIONS

This paper demonstrates that a two-step learning-based optimal control theory technique applied to dynamical maps allows one to determine the control necessary to stabilize chaotic dynamics or maintain chaos. The algorithm operates by drawing on a repertoire of learned controls that operates in a window around the unstable periodic points to keep the dynamics around this region. An important component of the learning process with the reference map is the introduction of noise to assure a measure of robustness to laboratory uncertainty. If the state is outside of this region, then the control algorithm attempts to retain order, but divergence will appear at high values of noise or uncertainty in the state or map parameters. This approach was shown to be reasonably robust to different noise ensembles consisting of changes in the initial conditions, errors in the optimal control sequence and uncertainty in the map parameters. Also the number of control configurations (i.e., computer experiments) is not directly related to the dimensionality of the system, suggesting that this method can be applied to complex systems.

## ACKNOWLEDGMENTS

J. B. would like to express his gratitude to Professor Ingrid Daubechies and Professor Yannis Kevrekidis for many interesting discussions. We acknowledge support from the Office of Naval Research and the U.S. Army Research Office.

[1] E. Ott, C. Grebogi, and J. A. Yorke, Phys. Rev. Lett. **64**, 1196 (1990); L. Poon and C. Grebogi, *ibid.* **75**, 4023 (1995), and references therein.

[2] S. J. Schiff, K. Jerger, D. H. Duong, T. Chang, M. L. Spano, and W. L. Ditto, Nature (London) **370**, 615 (1994), and references therein.

[3] K. Pyragas, Phys. Lett. A **180**, 99 (1992); K. Pyragas and A. Tamasevicius, Phys. Lett. A **180**, 99 (1993); W. Just, T. Bernard, M. Ostheimer, E. Reibold, and H. Benner, Phys. Rev. Lett. **78**, 203 (1997).

[4] D. T. Kaplan, Physica A **73**, 38 (1994).

[5] V. Petrov, E. Mihaliuk, S. K. Scott, and K. Showalter, Phys. Rev. E **51**, 3988 (1995).

[6] R. Chacon, Phys. Rev. Lett. **77**, 482 (1997).

[7] J. Botina and H. Rabitz, Phys. Rev. Lett. **75**, 2948 (1995); W. S. Warren, H. Rabitz, and M. Dahleh, Science **259**, 1588 (1994).

[8] W. Yang, M. Ding, A. J. Mandell, and E. Ott, Phys. Rev. E **51**, 102 (1995).

[9] Note that, in the learning process, one may think of $\xi_n$ as ''deterministic'' noise in that a single noise trajectory is employed; this causes no problem, as the system typically samples the same region of the state space many times.

[10] D. Ruelle, Phys. Today **46**(7), 24 (1994), and references therein; T. Chang, S. J.Schiff, T. Sauer, J.-P. Gossard, and R. E. Burke, Biophys. J. **67**, 671 (1994); V. In, S. E. Mahan, W. L. Ditto, and M. L. Spano, Phys. Rev. Lett. **74**, 4420 (1995).

[11] M. Klein and G. Baier, Chaos Solitons Fractals **4**, 1889 (1994).